Viscous scattering of a pressure wave: Calculation of the fluid tractions on a biomimetic acoustic velocity sensor

Dorel Homentcovschi[a] and Ronald N. Miles
Department of Mechanical Engineering, SUNY Binghamton, New York, 13902-6000

(Received 28 June 2005; revised 1 November 2005; accepted 9 November 2005)

In the paper we give a method for calculating the tractions (local forces) of the fluid motion determined by an incoming plane pressure wave on an artificial hair cell transducer structure. The sensing element of the transducer is a standing high aspect ratio cilium in the shape of a narrow thin curved beam (tape-like), which can be easily fabricated in micro-/nanotechnology. The method is based on considering the system of partial differential equations describing the motion of the compressible viscous fluid in an acoustic linearized approximation, and representation of the velocity field as a viscous acoustic single-layer potential. The boundary conditions, stating the cancellation of the velocity components on the solid beam, yield a two-dimensional (2-D) system of three integral equations over the beam's surface for the traction components. In the case of a narrow cilium, the system of integral equations furnishes a system of two 1-D integral equations over the symmetry curve of the structure for obtaining the tangential and normal components of the traction. This system is solved numerically by a finite (boundary) element method. The numerical code written for solving the problem was applied to some particular structures. The last structure is similar to the trichobothrium of a spider *Cupiennius salei*. The results obtained show that the curvature of the hair is enhancing sensitivity to flows directed normal to the main shaft of the hair confirming the assertion of Barth *et al.* [Philos. Trans. R. Soc. London, Ser. B **340**, 445–461 (1993)]. [DOI: 10.1121/1.2146108]

PACS number(s): 43.20.Fn [TDM] Pages: 777–787

I. INTRODUCTION

Many insects can detect the low-velocity movement of the ambient air by means of hair sensilla that are deflected from the resting position by the air motion. The sensilla respond to the sound and wind as long as the frequency of the incoming signal is small. This is the case in crickets whose filiform cercal hairs vibrate in a sound field,[1] in caterpillars' that react to the airborne vibrations of an approaching predator by means of filiform hairs on the thorax,[2,3] in cockroaches and grasshoppers that can have thousands of filiform sensory hairs of various sizes used for detecting danger.[4] The spider's filiform hairs, also referred to as trichobothria, form spatial clusters and areas capable of detecting the magnitude, direction and frequency of airborne signals.[5,6]

Fish use lateral line sensors to monitor sounds under water.[7,8] The lateral line system consists of an array of distributed sensor nodes, each of them being a mechanoreceptor having as a basic element a vertical cilium attached to sensory cells. When the cilium of the hair cell is bent by the water flow, the displacement will induce output responses from the attached nerve cells.

Filiform hair systems attracted attention of several authors who derived and applied physical–mathematical models to describe the behavior of sensilla and their interaction with surrounding fluid motion. Substantial progress has been made in the understanding of the physics behind the working of individual sensory hairs. Shimozawa and Kanou[9] proposed a model of a hair as a slender linearly tapered cone. The viscous force acting on the hair shaft was obtained by using the Oseen's approximation for the drag force generated on a circular cylinder by a steady-state flow of a viscous fluid given by Imai.[10] A more realistic shape of hair receptors as elongated paraboloids was considered by Kumagai *et al.*[11]

Humphrey *et al.*[12] made an extensive critical examination of Shimozawa and Kanou's results[9] and proposed a mathematical model of the oscillatory motion of filiform hairs of all arthropods. The shape of the hair is assumed to be a straight, cylindrically shaped (rod-like) body of finite length and diameter. They used as the driving force on the hair shaft (driven by oscillating air motion) the same expression as the drag force generated on the rod of a solid pendulum swinging in stationary air, given by Stokes in 1851.[13] The Stokes's solution was obtained by solving the linearized system of Navier–Stokes equations (the Stokes's approximation). The numerical method developed by Humphrey *et al.*[12,14,15] solves a rigorously derived form of the equation for the conservation of angular momentum for a single hair; its estimation of the dynamic drag force is very informative.

The comparison of the measured properties of hair and air motion with the values predicted numerically by the theory developed by Barth *et al.*[16] showed very good agreement. The theoretical considerations are of a very general nature: they can be applied not only to different hair morphologies and hair mechanics but also to different media (air or water).[17–19]

[a]Permanent address: Polytechnica University, Applied Science Department & Institute of Mathematical Statistics and Applied Mathematics of Romanian Academy, Calea13 Septembrie #13, RO-76100, Bucharest, Romania. Electronic mail: homentco@binghamton.edu

The exhaustive analysis in Ref. 20 has shown that the use of the Stokes' approximation for computing the drag force gives better results than Oseen's model. The conclusion is that Oseen's approximation is not appropriate and is not used hereafter in approaching these problems.

In a recent physical and mathematical approach, Humphrey *et al.*[21] examined the relative importance of the various hair parameters in determining a hair's absolute sensitivity to medium flow as well as its frequency tuning. The effects of different parameters affecting the response of a hair-like medium flow detector are also given for hairs in water.[18,21,22]

As pointed out in Ref. 22, there are two major objectives of this work. The first is to uncover and understand the basic "design" principles underpinning the performance characteristics of filiform hairs by trying to understand how physics impacted the sensory ecology and adaptive evolution of the natural motion sensors. The second aim is to derive and implement realistic physical–mathematical models for these exquisitely sensitive natural sensors. A model that predicts the hair's response will expedite the design and fabrication of artificial sensors of similar function and characteristics. The value of the engineering approach to hair sensilla sensitive to medium flow is also underlined by the analysis by Shimozawa *et al.*[23] The conclusion in Barth *et al.*[24] is that the outstanding sensitivity seen in the neural response of cricket filiform hairs appear to represent the most sensitive biological sensors so far known.

A number of researchers have recognized the utility of the hair cell transducer structure and have applied MEMS techniques to produce microscale artificial hair cell sensors for sensing the perturbations of the air or water. [25–30] Microfabrication offers the benefits of high spatial resolution, fast time response, integrated signal processing and, finally, low costs.

We discuss the class of air- or water-sensing devices, based on the momentum transfer principle, using a vertical high aspect ratio cilium in the shape of a narrow thin curved beam (tape-like) which can be easily micromachined. This type of sensing element has not been found in nature, but the hope is that they can reproduce some of the hair's functions. The sensor's output is related to the direction and the intensity of the flow. By providing more than two sensors, with their cilia pointing in different directions, it is possible to identify the direction of the local air flow (or sound).[25] Practically, these artificial cell sensors are grouped in arrays of sensors with systematically varying frontal orientation and cilium shape.

In this paper we focus on the mechanical interaction of the air flow with individual hair-like sensors. When the motion of the ambient medium ranges in the domain of low velocities and the cross dimension of the body is smaller than the thickness of the viscous boundary layer of the supporting substrate, the force density acting on the hair (the traction) is dominated by the viscosity of the flow. The relation between the incoming sound or velocity field and the output of the sensor is obtained by first solving the equations of the motion of the viscous compressible fluid in the linear acoustic approximation with specified boundary conditions for the traction on the sensing element; the next step, which we are not considering here, is a structure deformation analysis under the known tractions. The model described here is tailored specially for determining the tractions (understood as local forces) on the tape-like sensors. The resultant forces (particularly the drag resulting by summing all the local forces) are strongly dependent on the geometry of the problem and are very different from that corresponding to rod-like sensilla found on insects. As a result, the numerical data obtained from this theory cannot be readily compared with those obtained in the above-cited papers. The validation of the theory can be done by comparing the theoretical results with experimental values obtained for artificial tape-like motion sensors. On the other hand, some qualitative results can be transferred between rod-like and tape-like sensors. Thus, the last example considered in this paper can be compared to results obtained for the trichobotrium of a spider *(Cupiennius salei)*. Our calculations support the assertion of Barth *et al.*[16] that the role of curvature on the sensing hairs is to enhance the sensitivity to flows directed normal to the main shaft of the hair.

Despite their simplicity, these "rudimentary" velocity sensors have an advantage over their very "sophisticated" inspiring natural sensors. While every natural hair shaft is a single sensing element (characterized by total drag force), for tape-like artificial sensors it is possible, depending on the detection technique, to obtain more data as local forces in different assigned points. This way the function of a cluster of natural hair sensors could be substituted by just a few artificial hair-sensing elements.

The solution of the linearized equations of viscous acoustics is developed as a single-layer viscous acoustical potential, which leads to a two-dimensional, regular Fredholm integral equation of the first kind for determining the tractions on the sensors' surface. Accounting for the fact that the beam is narrow, an asymptotic analysis of the integral equation yields a unidimensional integral equation. This technique is similar to that used to obtain the lifting line equation in classical aerodynamics.[32] This unidimensional integral equation is solved by a boundary (finite) element technique for the tractions in the direction of the normal (at the sensors' surface) and tangent to the sensors' middle curve. Based on these theoretical considerations a numerical code has been written and some results are provided in Sec. IV D.

II. EQUATIONS OF MOTION OF A VISCOUS COMPRESSIBLE FLUID IN LINEAR ACOUSTICS APPROXIMATION FOR HARMONIC OSCILLATIONS IN TIME

A. The equations of the motion of a viscous fluid in the linear acoustic approximation

If the coordinate system is chosen so that the unperturbed fluid is at rest, the first-order equations describing the isentropic flow of the gas can be written as[31,33,34]

$$\frac{1}{c_0^2}\frac{\partial}{\partial t}\frac{p'}{\rho_0} + \nabla \cdot \mathbf{v}' = 0, \tag{1}$$

$$\frac{\partial \mathbf{v}'}{\partial t}+\frac{1}{\rho_0}\nabla\cdot\sigma'=\mathbf{0}, \tag{2}$$

where p' and v' denote the pressure and velocity perturbations, σ' is the stress tensor that in the case of Newtonian fluids has the expression

$$\sigma'_{ij}\equiv\sigma_{ij}[p',\mathbf{v}']=\left[p'-\left(\mu_B-\frac{2}{3}\mu\right)\nabla\cdot\mathbf{v}'\right]\delta_{ij} -\mu\left(\frac{\partial v'_i}{\partial x_j}+\frac{\partial v'_j}{\partial x_i}\right) \tag{3}$$

ρ_0, c_0 are the density and velocity of sound in a nonperturbed fluid, and by μ and μ_B we denote the shear and bulk viscosities.

The above equations are associated with the nonslip boundary condition

$$\mathbf{v}'=0, \quad \text{on } \mathcal{S}, \tag{4}$$

where the solid surfaces $\mathcal{S}$ limit the flow domain $\mathcal{D}$. Thus, the principal element to be determined by solving a viscous acoustical problem is the velocity field (a vectorial unknown field).

B. The basic equation in the case of harmonic oscillations in time

We consider the case where all the physical variables are harmonic in time with the same angular velocity $\omega=2\pi f$. The case of the general time dependence can be obtained, after analyzing each frequency separately, by Fourier superposition. In the case of simple harmonic oscillations in time we shall write

$$\{p'(\mathbf{x},t),\mathbf{v}'(\mathbf{x},t),\sigma'(\mathbf{x},t)\}=\{p(\mathbf{x}),\mathbf{v}(\mathbf{x}),\sigma(\mathbf{x})\}\exp(-i\omega t),$$

In this case, the continuity equation (1) becomes

$$\nabla\cdot\mathbf{v}=\frac{i\omega}{c_0^2}\frac{p}{\rho_0}. \tag{5}$$

Also, the momentum conservation equation can be written as

$$-i\omega\mathbf{v}+\frac{1}{\rho_0}\nabla\cdot\sigma=\mathbf{0}, \tag{6}$$

which in the case of Newtonian fluids becomes

$$\Delta\mathbf{v}+\frac{i\omega}{\nu}\mathbf{v}=\beta\nabla\frac{p}{\varrho_0}. \tag{7}$$

Here we have denoted

$$\beta=\frac{\rho_0-(\mu/3+\mu_B)i\omega/c_0^2}{\mu}.$$

The relationships (5) and (7) give the equation for the pressure,

$$[\Delta+k^2]p=0, \tag{8}$$

which in the case $\mu=\mu_B=0$ coincides with the basic equation determining the motion of the inviscid compressible fluid in the linear acoustic approximation. Finally, by applying the operator of Eq. (8) to Eq. (7), there results the basic equation describing the motion of the viscous compressible fluid in linear acoustic approximation,

$$[\Delta+k^2][\Delta+k^{*2}]\mathbf{v}=\mathbf{0}. \tag{9}$$

Here we have used the notations

$$k=\frac{\omega}{\sqrt{c_0^2-i\omega(4\mu/3+\mu_B)/\rho_0}}, \quad k^*=\sqrt{\frac{i\omega\rho_0}{\mu}},$$
$$\mathrm{Im}(k,k^*)\geq 0.$$

It is to be noticed that Eq. (8) is a Helmholtz-type equation and the operator in Eq. (9) is a product of two Helmholtz-type operators. Consequently, the velocity can be written as a sum of two terms: the first describes a propagation mode (also called the acoustical mode) and the second is a diffusion mode driven by viscosity.

C. Plane wave solution in the whole space

Consider an incoming pressure plane wave,

$$p^{\mathrm{in}}(\mathbf{x})=\rho_0c_0^2P_0\exp\{ik\mathbf{n}\cdot\mathbf{x}\}, \tag{10}$$

where $\mathbf{n}$ is the unit vector of the propagating direction and P_0 is a dimensionless constant used for scaling the amplitude of the incoming wave. It can be verified directly that (10) satisfies the basic pressure equation. Since the pressure field has an assigned form, Eq. (7) will determine the associated velocity field as

$$\mathbf{v}^{\mathrm{in}}(\mathbf{x})=ik\delta c_0^2p_0\mathbf{n}\exp\{ik\mathbf{n}\cdot\mathbf{x}\}, \tag{11}$$

where

$$\delta=\frac{\rho_0-(4\mu/3+\mu_B)i\omega/c_0^2}{i\omega\rho_0-\mu k^2}.$$

We notice that in this case that the velocity field contains only a propagating mode.

D. Plane wave solution in the half-space

Let us consider now the domain $\mathcal{D}$ as being the upper half-space $z>0$. The $z=0$ plane is assumed a solid boundary, hence the solution has to satisfy the no-slip boundary condition

$$\mathbf{v}(x,y,0)=0. \tag{12}$$

In the case the incident wave has the form

$$p^{\mathrm{in}}(\mathbf{x})=\rho_0c_0^2P_0\exp\{ik\mathbf{n}\cdot\mathbf{x}\}, \quad n_z\neq 0; \tag{13}$$

we consider the pressure field of the form

$$p(\mathbf{x})=\rho_0c_0^2P_0[\exp\{ik\mathbf{n}\cdot\mathbf{x}\}+A\exp\{ik\mathbf{n}'\cdot\mathbf{x}\}], \tag{14}$$

where $\mathbf{n}=(n_x,n_y,n_z)$, $\mathbf{n}'=(n_x,n_y,-n_z)$, and A is a constant. By using formula (11) we can write

$$\mathbf{v}(\mathbf{x})=ik\delta c_0^2P_0[\mathbf{n}\exp\{ik\mathbf{n}\cdot\mathbf{x}\}+A\mathbf{n}'\exp\{ik\mathbf{n}'\cdot\mathbf{x}\}] +\mathbf{u}^0c_0^2P_0\exp[ik(n_xx+n_yy)-qz], \tag{15}$$

where

$$q=\sqrt{k^2(n_x^2+n_y^2)-k^{*2}}, \quad \mathrm{Re}(q)>0.$$

The constants A and $\mathbf{u}^0$ are determined such that the solution satisfies the nonslip boundary condition:

$$A=\frac{qn_z-ik(n_x^2+n_y^2)}{qn_z+ik(n_x^2+n_y^2)},$$

$$u_x^0=\frac{-2ikq\delta n_x n_z}{qn_z+ik(n_x^2+n_y^2)},\quad u_y^0=\frac{-2ikq\delta n_y n_z}{qn_z+ik(n_x^2+n_y^2)},$$
$$u_z^0=\frac{2k^2\delta(n_x^2+n_y^2)n_z}{qn_z+ik(n_x^2+n_y^2)}. \tag{16}$$

It should be noted that the complementary velocity $\mathbf{u}=\mathbf{u}^0c_0^2P_0\exp[ik(n_xx+n_yy)-qz]$ has a boundary layer structure.

In the solution (14), (15) one can recognize the incident wave (the first term in brackets), the reflected wave (the second term), and the contribution of the viscous boundary layer (the last term). Consequently, the solution in this case contains a propagating mode and also a diffusive (viscous) mode. Also, relation (16) yields the refection coefficient for the acoustic pressure. The solution of the problem of reflection of a transverse wave from a flat boundary in the case of an incompressible fluid can be found in Ref. 35. The most important property of the reflected wave is that its amplitude decreases exponentially as the distance from the solid surface increases.

III. THE FUNDAMENTAL FORMULA AND THE BOUNDARY INTEGRAL EQUATION FOR THE MOTION OF A VISCOUS COMPRESSIBLE FLUID IN THE LINEAR ACOUSTIC APPROXIMATION

A. The fundamental formula

We assume that the body occupying the domain $\mathcal{D}^+$ limited by the surface $\mathcal{S}$ is immersed into an external flow field characterized by the pressure $p^0(\mathbf{x})$ and velocity $\mathbf{v}^0(\mathbf{x})$ that are solutions of the equations of the linearized viscous acoustics. These functions can be the plane wave solution in the whole space or that corresponding to the half-space $z>0$. The solution of the problem $[p(\mathbf{x}),\mathbf{v}(\mathbf{x})]$ is defined in the external domain $\mathcal{D}^-$.

It is possible to use a direct approach to solve the boundary-value problem by means of the finite difference or finite element methods. Due to the infinity of the domain these equations will be written for all the mesh points inside domain $\mathcal{D}^-$. We prefer a boundary integral formulation that involves more mathematics but results in a much simpler system of equations written only on the mesh points on the sensor's surface. The starting elements are the following integral relationships that are proved in the Appendix:

$$\gamma p(\mathbf{x})=p^0(\mathbf{x})-\nabla\cdot\int\int_{\mathcal{S}}\frac{\mathbf{t}(\mathbf{x}')\exp(ik|\mathbf{x}-\mathbf{x}'|)}{4\pi(1-i\omega\nu'/c_0^2)|\mathbf{x}-\mathbf{x}'|}da',$$

$$\gamma\mathbf{v}(\mathbf{x})=\mathbf{v}^0(\mathbf{x})+\int\int_{\mathcal{S}}\frac{\mathbf{t}(\mathbf{x}')\exp(ik^*|\mathbf{x}-\mathbf{x}'|)}{4\pi\rho_0\nu|\mathbf{x}-\mathbf{x}'|}\times da'+\nabla\nabla\cdot\int\int_{\mathcal{S}}\times\frac{\mathbf{t}(\mathbf{x}')[\exp(ik^*|\mathbf{x}-\mathbf{x}'|)-\exp(ik|\mathbf{x}-\mathbf{x}'|)]}{4\pi i\omega\rho_0|\mathbf{x}-\mathbf{x}'|}da'. \tag{17}$$

By da' we denoted the surface area element with respect to variable $\mathbf{x}'$ on the surface $\mathcal{S}$. Once the traction $\mathbf{t}(\mathbf{x}')$ on the boundary surface $\mathcal{S}$ is known, these relationships enable us to determine the velocity and pressure in any point in the domain $\mathcal{D}^-$. Since in the case of viscous fluids the boundary conditions on hard bodies are expressed in terms of velocities, the relationship (17) will be used more often. This is why we call this equation *the fundamental integral formula.*

Remark 1: In obtaining the relationship (17) *we have used the condition of no slip of the fluid along the surface* $\mathcal{S}$ (4). *This is why we have in formula* (17) *only a single-layer viscous acoustic potential.*

The fundamental formula can also be written as

$$\gamma\rho_0i\omega\mathbf{v}(\mathbf{x})=\rho_0i\omega\mathbf{v}^0(\mathbf{x})+\int\int_{\mathcal{S}}\frac{\mathbf{t}(\mathbf{x}')}{4\pi|\mathbf{x}-\mathbf{x}'|}\times A(|\mathbf{x}-\mathbf{x}'|,k,k^*)da'+\int\int_{\mathcal{S}}\frac{(\mathbf{x}-\mathbf{x}')[\mathbf{t}(\mathbf{x}')\cdot(\mathbf{x}-\mathbf{x}')]}{4\pi|\mathbf{x}-\mathbf{x}'|^3}\times C(|\mathbf{x}-\mathbf{x}'|,k,k^*)da',$$

where

$$A(|\mathbf{x}|,k,k^*)=k^{*2}\exp(ik^*|\mathbf{x}|)-\frac{\exp(ik^*|\mathbf{x}|)}{|\mathbf{x}|^2}(1-ik^*|\mathbf{x}|)+\frac{\exp(ik|\mathbf{x}|)}{|\mathbf{x}|^2}(1-ik|\mathbf{x}|), \tag{18}$$

$$C(|\mathbf{x}|,k,k^*)=\frac{3\exp(ik^*|\mathbf{x}|)}{|\mathbf{x}|^2}\left(1-ik^*|\mathbf{x}|-\frac{k^{*2}|\mathbf{x}|^2}{3}\right)-\frac{3\exp(ik|\mathbf{x}|)}{|\mathbf{x}|^2}\left(1-ik|\mathbf{x}|-\frac{k^2|\mathbf{x}|^2}{3}\right). \tag{19}$$

The behavior of the functions A and C for small values of $|\mathbf{x}|$ is given by formulas

$$A(|\mathbf{x}|,k,k^*)=\frac{1}{2}(k^2+k^{*2})+\frac{i|\mathbf{x}|}{3}(k^3+2k^{*3})$$
$$+O[(k^4+k^{*4})|\mathbf{x}|^2],$$
$$C(|\mathbf{x}|,k,k^*)=\frac{1}{2}(k^{*2}-k^2)+O[(k^4+k^{*4})$$
$$\times|\mathbf{x}|^2].$$

B. The boundary integral equation of the problem

By taking in the *fundamental integral formula* $\mathbf{x}=\mathbf{x}_0 \in S$ there results

$$\int\int_S \frac{(\mathbf{x}_0-\mathbf{x}')[\mathbf{t}(\mathbf{x}')\cdot(\mathbf{x}_0-\mathbf{x}')]}{4\pi|\mathbf{x}_0-\mathbf{x}'|^3}C(|\mathbf{x}_0-\mathbf{x}'|,k,k^*)da'$$
$$+\int\int_S \frac{\mathbf{t}(\mathbf{x}')}{4\pi|\mathbf{x}_0-\mathbf{x}'|}A(|\mathbf{x}_0-\mathbf{x}'|,k,k^*)da'$$
$$+i\omega\rho_0\mathbf{v}^0(\mathbf{x}_0)=0. \tag{20}$$

This is a Fredholm integral equation of the first kind for determining the boundary traction $\mathbf{t}(\mathbf{x})$. Analytical solutions of this equation can be obtained only in very particular cases. Therefore, it has to be solved numerically by boundary-element-type methods.

It is clear that the kernel of (20) has a singularity for $\mathbf{x}'=\mathbf{x}_0$. The singular part of the integral operator can be written as

$$\mathrm{I}[\mathbf{t}]=\frac{1}{2}(k^2+k^{*2})\int\int_S \frac{\mathbf{t}(\mathbf{x}')}{|\mathbf{x}_0-\mathbf{x}'|}da'$$
$$+\frac{1}{2}(k^{*2}-k^2)\int\int_S \frac{(\mathbf{x}_0-\mathbf{x}')[\mathbf{t}'\cdot(\mathbf{x}_0-\mathbf{x}')]}{|\mathbf{x}_0-\mathbf{x}'|^3}da'.$$

This form shows that when S is a Lyapunov surface, the kernels are weakly singular. For $\omega=0$ the equation (20) reduces to the Oseen operator for the viscous incompressible flow in Stokes' approximation. Consequently, the methods used to approximate the solution in the case of viscous incompressible fluids[37] can be successfully applied for integrating Eq. (20).

IV. CALCULATION OF THE TRACTION ON A LOW-FREQUENCY SENSOR

A. The integral equation of the curvilinear sensor approximation

We consider now the case of a low-frequency sensor having the shape of a curved narrow thin beam, symmetrical with respect to the plane $x=0$, of length L and width $2d_0g(s)$ [$g(s)$ being a given function, $|g(s)|\leqslant 1$] such that $\varepsilon=d_0/L\ll 1$. The range of frequencies considered here is $0.1<f<500$ Hz. At these frequencies the wavelength is large compared with the length L. The equation of the surface S is assumed of the form

$$y=y(s),\quad 0\leqslant s\leqslant L,$$
$$z=z(s),\quad 0\leqslant s\leqslant L,$$
$$x=x,\quad -d_0g(s),\leqslant x\leqslant d_0g(s).$$

This shape of the sensing element was chosen since it can be obtained in micro-/nanofabrication technology. Denote by C the central curve of the surface (Fig. 1), supposed to be contained in the plane $x=0$, and s is the curvilinear abscissa along C. We shall write the integral equation (20) for the points $\mathbf{x}_0$ along the curve C.

Also, we introduce dimensionless independent variables taking d_0 as the reference length along the x axis and L for the other directions. We also denote by capital letters the vector components orthogonal to the $\hat{x}$ direction. (By $\hat{\mathbf{v}}$ we denote the unit vector corresponding to the direction of vector $\mathbf{v}$.) Thus, we have

$$\mathbf{x}\to L(\varepsilon x\hat{\mathbf{x}}+\mathbf{R}),\quad \mathbf{R}=(0,y/L,z/L),$$
$$|\mathbf{x}_0-\mathbf{x}'|\to L\{\varepsilon^2x'^2+|\mathbf{R}_0-\mathbf{R}'|^2\}^{1/2},$$
$$\mathbf{t}=t_x\hat{\mathbf{x}}+\mathbf{T},\quad \mathbf{v}^0=v_x^0\hat{\mathbf{x}}+\mathbf{V}^0,$$
$$da'=\varepsilon L^2\,dx'\,ds'.$$

Since the surface is narrow and the kernel of the integral equation is an even function with respect to x', the system of integral equations (20) is separable into an equation corresponding to the x direction,

$$v_x^0(\mathbf{R}_0)+\int\int_S \frac{t_x(\mathbf{R}')}{4\pi\rho_0|\mathbf{x}_0-\mathbf{x}'|}A(|\mathbf{x}_0-\mathbf{x}'|,\omega,\nu)da'$$
$$+O(L^2\varepsilon^3)=0, \tag{21}$$

and a vectorial equation (a system of two integral equations) for the other directions,

$$\mathbf{V}^0(\mathbf{R}_0)+\int\int_S \frac{\mathbf{T}(\mathbf{R}')}{4\pi\rho_0|\mathbf{x}_0-\mathbf{x}'|}A(|\mathbf{x}_0-\mathbf{x}'|,\omega,\nu)da'$$
$$+L^2\int\int_S \frac{(\mathbf{R}_0-\mathbf{R}')[\mathbf{T}(\mathbf{R}')\cdot(\mathbf{R}_0-\mathbf{R}')]}{4\pi\rho_0|\mathbf{x}_0-\mathbf{x}'|^3}$$
$$\times C(|\mathbf{x}_0-\mathbf{x}'|,\omega,\nu)da'+O(L^2\varepsilon^3)=\mathbf{0}. \tag{22}$$

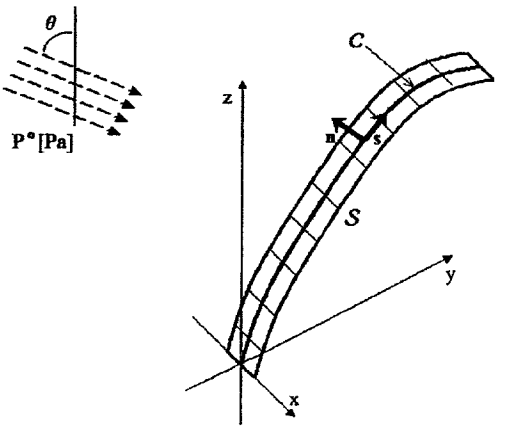

FIG. 1. The geometry of a sensing element.

We shall solve the system (22), which gives the main forces on the sensor surface. Let $F(\mathbf{x}')$ be a smooth function. We can write

$$F(\mathbf{x}') = F(\mathbf{R}') + x'\,\partial_1 F(\mathbf{R}') + O(\varepsilon^2),$$

and hence,

$$\int_{-d_0 g(s)}^{d_0 g(s)} \frac{F(\mathbf{x}')}{|\mathbf{x}_0 - \mathbf{x}'|} dx' = 2\int_0^{d_0 g(s)} \frac{F(\mathbf{R}')}{|\mathbf{x}_0 - \mathbf{x}'|} dx' + O(\varepsilon^3) = 2F(\mathbf{R}')\log\frac{\varepsilon g(s) + \sqrt{\varepsilon^2 g^2(s) + |\mathbf{R}_0 - \mathbf{R}'|^2}}{|\mathbf{R}_0 - \mathbf{R}'|} + O(\varepsilon^3),$$

$$L^2 \int_{-d_0 g(s)}^{d_0 g(s)} \frac{F(\mathbf{x}')}{|\mathbf{x}_0 - \mathbf{x}'|} dx' = \frac{2\varepsilon g(s) F(\mathbf{R}')}{|\mathbf{R}_0 - \mathbf{R}'|^2} \frac{1}{\sqrt{\varepsilon^2 g^2(s) + |\mathbf{R}_0 - \mathbf{R}'|^2}} + O(\varepsilon^3).$$

Taking into consideration these formulas, the integration with respect to x' in Eqs. (21) and (22) can be performed directly, and there results

$$2\pi\rho_0 \mathbf{V}^0(\mathbf{R}_0) + \int_C \mathbf{T}(\mathbf{R}') A(|\mathbf{R}_0 - \mathbf{R}'|) \times \log\frac{\varepsilon g(s)' + \sqrt{\varepsilon^2 g^2(s') + |\mathbf{R}_0 - \mathbf{R}'|^2}}{|\mathbf{R}_0 - \mathbf{R}'|} ds' + \varepsilon \int_C \frac{\mathbf{R}' - \mathbf{R}_0}{|\mathbf{R}' - \mathbf{R}_0|} \left(\mathbf{T}(\mathbf{R}') \cdot \frac{\mathbf{R}' - \mathbf{R}_0}{|\mathbf{R}' - \mathbf{R}_0|} \right) \times \frac{C(|\mathbf{R}_0 - \mathbf{R}'|)}{\sqrt{\varepsilon^2 g^2(s') + |\mathbf{R}_0 - \mathbf{R}'|^2}} g(s)' ds' = \mathbf{0}, \tag{23}$$

which is the integral equation for determining the traction on the low-frequency sensor.

Remark 2: In the above formulas it was assumed that the tractions are smooth functions across the beam. Equation (23) *still proves true in the case the tractions* $T(\mathbf{x}')$ *have integrable singularities (like square root singularities) at the beam's sharp edges but is a smooth function at all the other points.*

B. A boundary-element approach to the integral equation of the curvilinear sensor

For a numerical solution of Eq. (23) we consider the nodal points $\mathbf{R}_j^0$, $j=1,\ldots,N+1$ on the curve C and approximate the arc C_j between the points $\mathbf{R}_j^0$ and $\mathbf{R}_{j+1}^0$ of the curve by the line segment $\mathcal{E}_j \equiv \overline{\mathbf{R}_j^0 \mathbf{R}_{j+1}^0}$, which is the basic boundary element we will use. The length of this line segment is denoted by h_j. We shall determine the solution of the equation in the points $\mathbf{R}_j = (\mathbf{R}_j^0 + \mathbf{R}_{j+1}^0)/2$ lying at the middle of the boundary elements. Also, for the vectorial quantities (like velocities and tractions) we consider local Cartesian systems of coordinates given by the unit vector $\hat{\mathbf{s}}_j$ of the direction $\overrightarrow{\mathbf{R}_j^0 \mathbf{R}_{j+1}^0}$ and the normal unit vector $\hat{\mathbf{n}}_j$. We consider the traction $\mathbf{T}(\mathbf{R}')$ as constant along the boundary element $\mathcal{E}_j$ and equal to the value

$$\mathbf{T}_j = \mathbf{T}(\mathbf{R}_j) = T_j^s \hat{\mathbf{s}}_j + T_j^n \hat{\mathbf{n}}_j,$$

and will write the equation (23) in the points $\mathbf{R}_k$ projected on a local system of coordinates in the form

$$\sum_{j=1}^N M_{kj}^{nn} T_j^n + \sum_{j=1}^N M_{kj}^{ns} T_j^s = -2\pi i\omega\rho_0 V_k^{0n}/\varepsilon, \tag{24}$$

$$\sum_{j=1}^N M_{kj}^{sn} T_j^n + \sum_{j=1}^N M_{kj}^{ss} T_j^s = -2\pi i\omega\rho_0 V_k^{0s}/\varepsilon, \tag{25}$$

where

$$M_{kj}^{nn} = \hat{\mathbf{n}}_k \cdot \hat{\mathbf{n}}_j I_{kj} + J_{kj}[\hat{\mathbf{n}}_k, \hat{\mathbf{n}}_j], \quad M_{kj}^{ns} = [\hat{\mathbf{n}}_k \cdot \hat{\mathbf{s}}_j I_{kj} + J_{kj}[\hat{\mathbf{n}}_k, \hat{\mathbf{s}}_j]], \quad j,k = 1,\ldots,N,$$

$$M_{kj}^{sn} = \hat{\mathbf{s}}_k \cdot \hat{\mathbf{n}}_j I_{kj} + J_{kj}[\hat{\mathbf{s}}_k, \hat{\mathbf{n}}_j], \quad M_{kj}^{ss} = \hat{\mathbf{s}}_k \cdot \hat{\mathbf{s}}_j I_{kj} + J_{kj}[\hat{\mathbf{s}}_k, \hat{\mathbf{s}}_j], \quad j,k = 1,\ldots,N.$$

Here we have denoted

$$I_{kj} = \frac{1}{\varepsilon} A(|\mathbf{R}_j - \mathbf{R}_k|) \int \log\frac{\varepsilon g_j + \sqrt{\varepsilon^2 g_j^2 + |\mathbf{R}' - \mathbf{R}_k|^2}}{|\mathbf{R}' - \mathbf{R}_k|} ds', \tag{26}$$

$$\mathbf{J}_{kj}[\mathbf{a}_j] = C(|\mathbf{R}_j - \mathbf{R}_k|) g_j \int \frac{\mathbf{R}' - \mathbf{R}_k}{|\mathbf{R}' - \mathbf{R}_k|} \left(\frac{\mathbf{R}' - \mathbf{R}_k}{|\mathbf{R}' - \mathbf{R}_k|} \cdot \mathbf{a}_j \right) \times \frac{ds'}{\sqrt{\varepsilon^2 g_j^2 + |\mathbf{R}' - \mathbf{R}_k|^2}} \tag{27}$$

$$J_{kj}[\hat{\mathbf{s}}_k, \hat{\mathbf{n}}_j] = \hat{\mathbf{s}}_k \cdot \mathbf{J}_{kj}[\hat{\mathbf{n}}_j]; \quad J_{kj}[\hat{\mathbf{n}}_k, \hat{\mathbf{n}}_j] = \hat{\mathbf{n}}_k \cdot \mathbf{J}_{kj}[\hat{\mathbf{n}}_j],$$

$$J_{kj}[\hat{\mathbf{s}}_k, \hat{\mathbf{s}}_j] = \hat{\mathbf{s}}_k \cdot \mathbf{J}_{kj}[\hat{\mathbf{s}}_j]; \quad J_{kj}[\hat{\mathbf{n}}_k, \hat{\mathbf{s}}_j] = \hat{\mathbf{n}}_k \cdot \mathbf{J}_{kj}[\hat{\mathbf{s}}_j].$$

1. Calculation of the integrals I_{kj}, J_{kj} for $k \neq j$

To compute the integrals (26) and (27) for $j \neq k$, we use an asymptotic expansion around $\varepsilon=0$ and evaluate analytically the resulting integrals. Neglecting $O(\varepsilon^2)$ terms there results

$$I_{kj} = A(|\mathbf{R}_j - \mathbf{R}_k|) g_j I_1,$$

$$\mathbf{J}_{kj}[\mathbf{a}_j] = C(|\mathbf{R}_j - \mathbf{R}_k|) g_j [a_j^t \hat{\mathbf{s}}_j I_1 + R_{jk}^n (a_j^n \hat{\mathbf{s}}_j + a_j^t \hat{\mathbf{n}}_j) I_2 + (-a_j^t \hat{\mathbf{s}}_j + a_j^n \hat{\mathbf{n}}_j) I_3].$$

Here we have used the notations

$$R_{jk}^t = (\mathbf{R}_j - \mathbf{R}_k) \cdot \hat{\mathbf{s}}_j, \quad R_{jk}^n = (\mathbf{R}_j - \mathbf{R}_k) \cdot \hat{\mathbf{n}}_j,$$

$$\mathbf{a}_j = a_j^t \hat{\mathbf{s}}_j + a_j^n \hat{\mathbf{n}}_j.$$

The integrals I_1, I_2, I_3 have the expressions

$$I_1 = \log \frac{R^+ + R_{jk}^t + h_j/2}{R^- + R_{jk}^t - h_j/2},$$

$$I_2 = \frac{2R_{jk}^t h_j}{R^+ R^- (R^+ + R^-)},$$

$$I_3 = \frac{h_j}{R^+ R^- (R^+ + R^-)} \left((R_{jk}^n)^2 - (R_{jk}^t)^2 + \left(\frac{h_j}{2}\right)^2 + R^+ R^- \right),$$

$$R^+ = \left| \sqrt{(R_{jk}^t + h_j/2)^2 + (R_{jk}^n)^2} \right|,$$

$$R^- = \left| \sqrt{(R_{jk}^t - h_j/2)^2 + (R_{jk}^n)^2} \right|.$$

2. Calculation of the integrals I_{kk}, J_{kk}

By performing the change of variables,

$$\mathbf{R}_k' = \mathbf{R}_k^0 + \left(\frac{1}{2} + \frac{t}{h_k}\right)(\mathbf{R}_{k+1}^0 - \mathbf{R}_k^0),$$

the integrals I_{kk} and J_{kk} become

$$I_{kk} = \frac{A(0)}{\varepsilon} \int_{-h_k/2}^{h_k/2} \log \frac{\varepsilon g_k + \sqrt{[\varepsilon g_k]^2 + t^2}}{|t|} dt = 2A(0) g_k \int_0^{h_k/(2\varepsilon g_k)} \log \frac{1 + \sqrt{1+v^2}}{v} dv. \quad (28)$$

We have

$$J_{kk}[\hat{\mathbf{n}}_k, \hat{\mathbf{n}}_k] = J_{kk}[\hat{\mathbf{s}}_k, \hat{\mathbf{n}}_k] = J_{kk}[\hat{\mathbf{n}}_k, \hat{\mathbf{s}}_k] = 0$$

and

$$J_{kk}[\hat{\mathbf{s}}_k, \hat{\mathbf{s}}_k] = C(0) g_k \int_{-h_k/2}^{h_k/2} \frac{dt}{\sqrt{[\varepsilon g_k]^2 + t^2}} = 2C(0) g_k \log \left[\frac{h_k}{2\varepsilon g_k} + \sqrt{1 + \left(\frac{h_k}{2\varepsilon g_k}\right)^2} \right]. \quad (29)$$

The integral in formula (28) will be evaluated numerically.

Remark 3: We note that in formulas (28)–(29) enters the ratio h_k/ε. In order to keep these terms finite, the number of elements has to be chosen such that this ratio is of order $O(1)$. This is the price paid for combining a small parameter asymptotic expansion with a finite element solution of the resulting integral equation.

C. A boundary-element approach for the curvilinear sensor approximation in a half-space

In the case where the domain is the half-space $z>0$ we will consider also the symmetrical curve C' of C with respect to the plane $z=0$. In the case we have on the whole curvilinear arc $C' \cup C$ a number of $2N$ linear boundary elements we can write the equations (24) and (25) taking $2N$ instead of N. Taking also in consideration that for symmetrical elements we have

$$T_j^n = T_{2N+1-j}^n, \quad T_j^s = -T_{2N+1-j}^s, \quad j = 1, \ldots, N.$$

The system of equations for determining the tractions on the surface become

$$\sum_{j=1}^{N} Q_{kj}^{nn} T_j^n + \sum_{j=1}^{N} Q_{kj}^{ns} T_j^s = -2\pi i \omega \rho_0 V_k^{0n}/\varepsilon, \quad k = 1, \ldots, N, \quad (30)$$

$$\sum_{j=1}^{N} Q_{kj}^{sn} T_j^n + \sum_{j=1}^{N} Q_{kj}^{ss} T_j^s = -2\pi i \omega \rho_0 V_k^{0s}/\varepsilon, \quad k = 1, \ldots, N, \quad (31)$$

where

$$Q_{kj}^{nn} = M_{kj}^{nn} + M_{k,2N+1-j}^{nn}, \quad Q_{kj}^{ns} = M_{kj}^{ns} - M_{k,2N+1-j}^{ns}, \quad j = 1, \ldots, N,$$

$$Q_{kj}^{sn} = M_{kj}^{sn} + M_{k,2N+1-j}^{sn}, \quad Q_{kj}^{ss} = M_{kj}^{ss} - M_{k,2N+1-j}^{ss}, \quad j = 1, \ldots, N.$$

The traction on the surface is determined by the values T_j^n, $T_j^s (j=1, \ldots, N)$ resulting by solving the system (30), (31).

Remark 4: We note that by taking also the symmetrical curve C' of C with respect to the $z=0$ plane we assure the cancellation of the normal velocity component along the z plane. The other two components are different from zero, but we expect them to be small due to the small perturbations produced by the sensor in the external domain. A complete solution has to consider also a traction (mechanical resistance) distribution along the plane $z=0$. But, the frictional resistance within the hair base can be assumed zero since, according to Ref. 20, no practical method is available to measure such slight mechanical resistance.

D. Application

The developed theory and formulas were implemented into a MATLAB program. Various parameters for the sound field and the description of the shape and dimensions of the sound sensors can be input into the program. The tractions at the specified points on the central curve will be the output. These output forces can be utilized in a finite element model to gauge the harmonic response of the sound sensor.

In all the applications, the constant P_0 has been chosen such that the incoming pressure wave has the amplitude 1 Pa; the frequency is assumed to be 100 Hz.

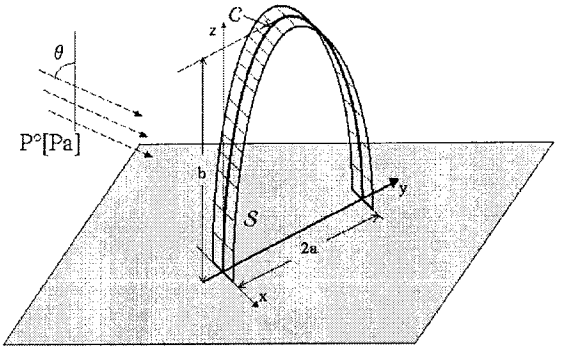

FIG. 2. A sensing element in the shape of a half-ellipse.

The program was tested on a half-elliptical shape sensor of 1 and 3.5 mm half-axis (Fig. 2) since it has two ends on the plane $z=0$ and a simple analytical expression. The width of the thin beam was chosen as 0.1 mm. The MATLAB program was run for three inclinations of the incident sound wave: $\theta=\pi/3, \pi/4, \pi/8$. The plots of the normal tractions are given in Fig. 3 and those of tangential tractions in Fig. 4. The continuous lines correspond to the real part of the tractions and the dotted line to the imaginary parts.

The next application contains the case of a vertical plane beam of variable width and a horizontal incoming plane wave ($\theta=\pi/2$) given in Fig. 5. Two cases were considered (1) ($a_1=0.01$ mm, $a_2=0.1$ mm) corresponding to a long trapezoid having its small basis in the plane $z=0$ and (2) ($a_1=0.1$ mm, $a_2=0.01$ mm) when the trapezoid has its big basis in the plane $z=0$. The moment of the forces resulting from normal tractions with respect to the $\mathcal{O}x$ axis are plotted in Fig. 6. The total moment is in the first case $MT_1=9.0\times10^{-8}-6.6\times10^{-9}i$(mm·N), and in the second case $MT_2=6.4\times10^{-8}-3.7\times10^{-9}i$(mm·N), which shows a strong influence of the shape of the thin beam on the moment. This is, in fact, the result of the action of the boundary layer on the plane $x\mathcal{O}y$. (The geometrical parameters of the beam in this case are: $L=1$ mm, *big basis* = 100 μm, *small basis* = 10 μm). Hence, for designing an artificial hair-cell sensor the first case would be preferable.

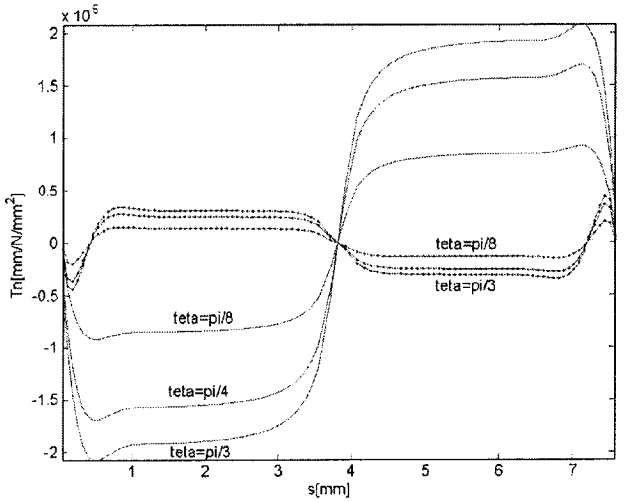

FIG. 3. The normal tractions for the sensing element in Fig. 2.

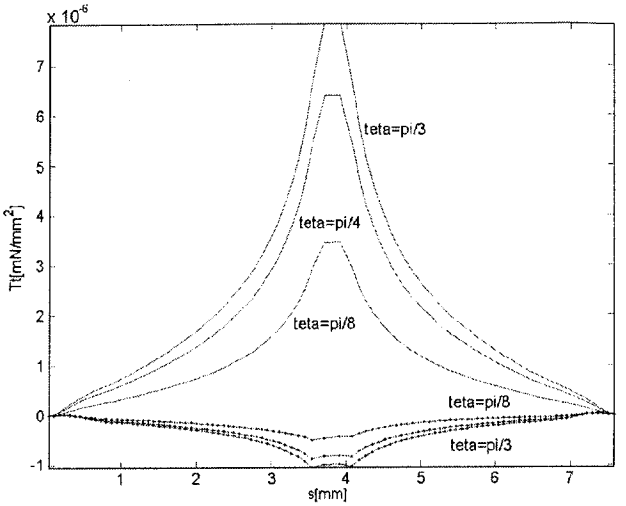

FIG. 4. The tangential tractions for the sensing element in Fig. 2.

Finally, the last application is that in Fig. 7, where we have a vertical rectangular narrow beam of length b that has attached at the upper end a horizontal rectangular beam of length a of the same width as the vertical beam. These beams are connected by a quarter of circle of radius r to ensure that the entire surface $\mathcal{S}$ is smooth. This structure is under the influence of a horizontal plane pressure wave of 1 Pa amplitude given by formula (15). For the case $a=8$ mm, $b=3$ mm, $r=0.1$ mm, and $width=0.14$ mm, the tractions on the structure are plotted in Fig. 8 (the real part) and in Fig. 9—the imaginary part. This structure is also advantageous for designing artificial hair-like sensors since all the force resulting from the tractions on the horizontal beam are acting on the upper end of the vertical beam, which will give a larger deflection of this component. This example is very similar to the trichobothrium of a spider *Cupiennius salei*. The curvature of the motion sensing hair is enhancing the sensitivity of the trichobothrium to flows normal to the main shaft of the hair. This fact supports the speculation by Barth *et al.* concerning the role of curvature in the sensing process.[16]

By reversing the direction of the incoming pressure wave the tractions in the last application remain unchanged. This can be considered as a result of the theorem (of Olmstead and Gautesen [38]) concerning the drag invariance for the

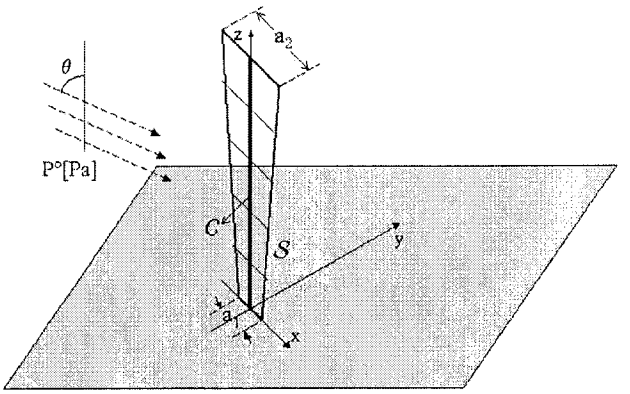

FIG. 5. The sensing element in the shape of an erected trapezoid.

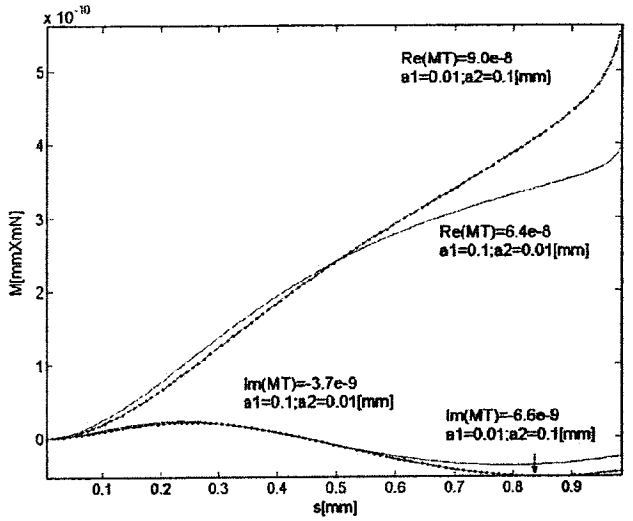

FIG. 6. The moment of normal tractions for the sensing element in Fig. 5 for two different geometries: the trapezoid having the small basis on the plane $z=0$ (dotted line) and the case the large basis is on the plane $z=0$ (simple continuous line).

reversal of the flow velocity for an arbitrary body. This paradox, proved in the case of incompressible flow, is still valid for the flow of a compressible viscous fluid in the linearized acoustic approximation.

In all the considered examples, the imaginary part of the tractions are much smaller than the real part, showing a strong influence of the viscosity.

ACKNOWLEDGMENTS

The careful, constructive suggestions of the reviewers is greatfully acknowledged. This work has been supported through a NIH Grant No. R01 DC05762-1A1 to RNM.

APPENDIX: THE FUNDAMENTAL INTEGRAL FORMULA

We shall assume that the body occupying the domain $\mathcal{D}^+$ limited by the surface $\mathcal{S}$ is immersed into an external flow field characterized by the pressure $p^0(\mathbf{x})$ and velocity $\mathbf{v}^0(\mathbf{x})$, which are satisfying the basic equations. The solution of the

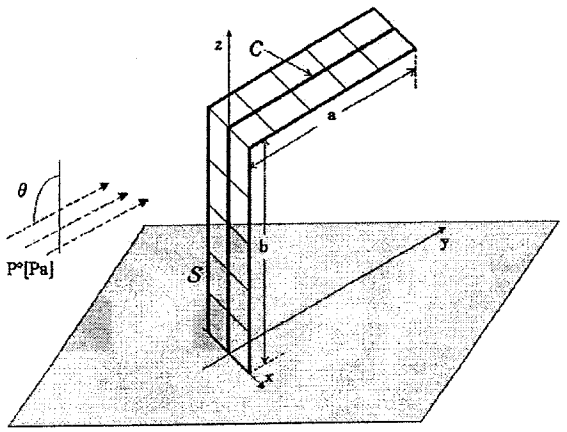

FIG. 7. The sensing element in the shape of a horizontal narrow beam attached at the upper end of a vertical beam.

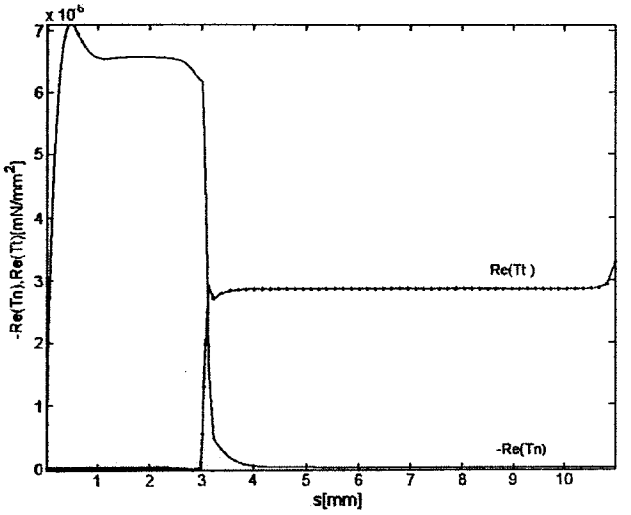

FIG. 8. The real part of normal tractions (continuous line) and the tangential tractions (dotted line) for the geometry in Fig. 7.

problem $[p(\mathbf{x}),\mathbf{v}(\mathbf{x})]$ is defined in the external domain $\mathcal{D}^-$. We extend these functions with the value 0 in domain $\mathcal{D}^+$. Then we have

$$\frac{-i\omega}{c_0^2}\frac{p^0}{\rho_0}+\nabla\cdot\mathbf{v}^0=0,\quad -i\omega\mathbf{v}^0+\frac{1}{\rho_0}\nabla\cdot\sigma^0=\mathbf{0},\quad \text{in } \mathcal{D}^+\cup\mathcal{S}\cup\mathcal{D}^-, \tag{A1}$$

$$\frac{-i\omega}{c_0^2}\frac{p}{\rho_0}+\nabla\cdot\mathbf{v}^0=0,\quad -i\omega\mathbf{v}+\frac{1}{\rho_0}\nabla\cdot\sigma=\mathbf{0},\quad \text{in } \mathcal{D}^+\cup\mathcal{D}^-. \tag{A2}$$

Also, we define

$$p^*=p-p^0,\quad \mathbf{v}^*=\mathbf{v}-\mathbf{v}^0,\quad \text{in } \mathcal{D}^+\cup\mathcal{D}^-, \tag{A3}$$

which, by means of relationships (A1), (A2) are satisfying the equations

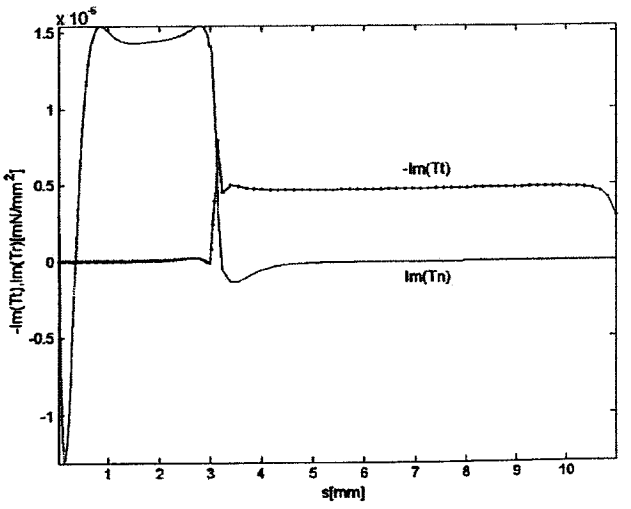

FIG. 9. The imaginary part of normal tractions (continuous line) and the tangential tractions (dotted line) for the geometry in Fig. 7.

$$\frac{-i\omega p^*}{c_0^2\ \rho_0}+\nabla\cdot\mathbf{v}^*=0,\quad -i\omega\mathbf{v}^*+\frac{1}{\rho_0}\nabla\cdot\sigma^*=\mathbf{0},\tag{A4}$$

in $\mathcal{D}^+\cup\mathcal{D}^-$.

Now, we consider the Fourier transform with respect to space variables,

$$\{\widetilde{p^*}(\mathbf{k}),\widetilde{\mathbf{v}^*}(\mathbf{k}),\widetilde{\sigma^*}(\mathbf{k})\}=\int\int\int\{p^*(\mathbf{x}),\mathbf{v}^*(\mathbf{x}),\sigma^*(\mathbf{x})\}\times\exp(-i\mathbf{k}\cdot\mathbf{x})dv_x;$$

which results in

$$\begin{aligned}\widetilde{\nabla\cdot\sigma^*}&=\int\int\int\nabla\cdot\sigma^*(\mathbf{x})\exp(-i\mathbf{k}\cdot\mathbf{x})dv_x\\&=\int\int\int_{\mathcal{D}^+}\nabla\cdot\sigma^*(\mathbf{x})\exp(-i\mathbf{k}\cdot\mathbf{x})dv_x\\&\quad+\int\int\int_{\mathcal{D}^-}\nabla\cdot\sigma^*(\mathbf{x})\exp(-i\mathbf{k}\cdot\mathbf{x})dv_x.\end{aligned}$$

But

$$\begin{aligned}\nabla\cdot\sigma^*\exp(-i\mathbf{k}\cdot\mathbf{x})&=\nabla\cdot[\sigma^*\exp(-i\mathbf{k}\cdot\mathbf{x})]\\&\quad-[\nabla\exp(-i\mathbf{k}\cdot\mathbf{x})]\cdot\sigma^*\\&=\nabla\cdot[\sigma^*\exp(-i\mathbf{k}\cdot\mathbf{x})]\\&\quad+i\mathbf{k}\cdot\sigma^*\exp(-i\mathbf{k}\cdot\mathbf{x}).\end{aligned}$$

Then, we obtain

$$\begin{aligned}&\int\int\int_{\mathcal{D}^+}\nabla\cdot\sigma^*(\mathbf{x})\exp(-i\mathbf{k}\cdot\mathbf{x})dv_x\\&=i\mathbf{k}\cdot\int\int\int_{\mathcal{D}^+}\sigma^*(\mathbf{x})\exp(-i\mathbf{k}\cdot\mathbf{x})dv_x\\&\quad-\int\int_{\mathcal{S}}\mathbf{n}\cdot\sigma^0(\mathbf{x})\exp(-i\mathbf{k}\cdot\mathbf{x})da,\end{aligned}\tag{A5}$$

$$\begin{aligned}&\int\int\int_{\mathcal{D}^-}\nabla\cdot\sigma^*(\mathbf{x})\exp(-i\mathbf{k}\cdot\mathbf{x})dv_x\\&=i\mathbf{k}\cdot\int\int\int_{\mathcal{D}^-}\sigma^*(\mathbf{x})\exp(-i\mathbf{k}\cdot\mathbf{x})dv_x\\&\quad-\int\int_{\mathcal{S}}\mathbf{n}\cdot[\sigma(\mathbf{x})-\sigma^0(\mathbf{x})]\exp(-i\mathbf{k}\cdot\mathbf{x})da,\end{aligned}\tag{A6}$$

where $\mathbf{n}$ denotes the unit normal vector at the surface $\mathcal{S}$ pointing outward. The sum of relationships (A5) and (A6) gives

$$\widetilde{\nabla\cdot\sigma^*}=-i\mathbf{k}\cdot\widetilde{\sigma^*}-\int\int_{\mathcal{S}}\mathbf{t}(\mathbf{x})\exp(-i\mathbf{k}\cdot\mathbf{x})da,$$

where

$$\mathbf{t}(\mathbf{x})=\mathbf{n}\cdot\sigma(\mathbf{x})$$

is the traction (surface stress) at the surface. For the velocity we obtain similarly

$$\widetilde{\nabla\cdot\sigma^*}=-i\mathbf{k}\cdot\widetilde{\mathbf{v}^*},$$

where the condition $\mathbf{v}=\mathbf{0}$ on the solid surface $\mathcal{S}$ has been used.

The Fourier transform of the system (A4) gives

$$\frac{-i\omega\widetilde{p^*}}{c_0^2\ \rho_0}+i\mathbf{k}\cdot\widetilde{\mathbf{v}^*}=0,\tag{A7}$$

$$-i\omega\widetilde{\mathbf{v}^*}+i\mathbf{k}\cdot\frac{1}{\rho_0}\widetilde{\sigma^*}=\frac{1}{\rho_0}\int\int_{\mathcal{S}}\mathbf{t}(\mathbf{x})\exp(-i\mathbf{k}\cdot\mathbf{x})da.\tag{A8}$$

Thus, the algebraic system obtained in Fourier Transform space contains also on the right-hand side of Eq. (A8) the action of the surface $\mathcal{S}$ on the fluid motion. Since we have

$$\widetilde{\sigma_{ij}^*}=\left[\widetilde{p^*}-\left(\mu_B-\frac{2}{3}\mu\right)i\mathbf{k}\cdot\widetilde{\mathbf{v}^*}\right]\delta_{ij}-\mu(ik_j\widetilde{v_i^*}+ik_i\widetilde{v_j^*}),$$

the equation (A8) can be written in the form

$$\begin{aligned}&(\nu|\mathbf{k}|^2-i\omega)\widetilde{\mathbf{v}^*}+i\mathbf{k}\cdot\left(\frac{\widetilde{p^*}}{\rho_0}-(\nu'-\nu)i\mathbf{k}\cdot\widetilde{\mathbf{v}^*}\right)\\&\quad=\frac{1}{\rho_0}\int\int_{\mathcal{S}}\mathbf{t}(\mathbf{x})\exp(-i\mathbf{k}\cdot\mathbf{x})da.\end{aligned}\tag{A9}$$

The inner product of the equation ( ) by $i\mathbf{k}$ gives

$$\begin{aligned}&(\nu'|\mathbf{k}|^2-i\omega)i\mathbf{k}\cdot\widetilde{\mathbf{v}^*}-|\mathbf{k}|^2\cdot\frac{\widetilde{p^*}}{\rho_0}=\frac{1}{\rho_0}\int\int_{\mathcal{S}}i\mathbf{k}\cdot\mathbf{t}(\mathbf{x})\\&\quad\times\exp(-i\mathbf{k}\cdot\mathbf{x})da.\end{aligned}\tag{A10}$$

The equations (A8), (A9), and (A10) can be solved for $\widetilde{p^*}$ and $\widetilde{\mathbf{v}^*}$,

$$\widetilde{p^*}(\mathbf{k})=\frac{1}{1-i\omega\nu'/c_0^2}\int\int_{\mathcal{S}}\frac{i\mathbf{k}\cdot\mathbf{t}(\mathbf{x})}{|\mathbf{k}|^2-k^2}\exp(-i\mathbf{k}\cdot\mathbf{x})da,\tag{A11}$$

$$\widetilde{\mathbf{v}^*}(\mathbf{k})=\frac{1}{\rho_0\nu}\int\int_{\mathcal{S}}\frac{\mathbf{t}(\mathbf{x})}{|\mathbf{k}|^2-k^{*2}}\exp(-i\mathbf{k}\cdot\mathbf{x})da\tag{A12}$$

$$\begin{aligned}&+\frac{1}{i\omega\rho_0}\int\int_{\mathcal{S}}\frac{i\mathbf{k}[i\mathbf{k}\cdot\mathbf{t}(\mathbf{x})]}{|\mathbf{k}|^2-k^{*2}}\exp(-i\mathbf{k}\cdot\mathbf{x})da\\&-\frac{1}{i\omega\rho_0}\int\int_{\mathcal{S}}\frac{i\mathbf{k}[i\mathbf{k}\cdot\mathbf{t}(\mathbf{x})]}{|\mathbf{k}|^2-k^2}\exp(-i\mathbf{k}\cdot\mathbf{x})da.\end{aligned}\tag{A13}$$

For determining the corresponding representation formulas in physical space, we shall use the inversion formula[33,36]

$$\frac{1}{(2\pi)^3}\int\int\int\frac{\exp(i\mathbf{k}\cdot\mathbf{x})}{|\mathbf{k}|^2-\lambda}dv_k=\frac{\exp(i\sqrt{\lambda}|\mathbf{x}|)}{4\pi|\mathbf{x}|},\tag{A14}$$

where $\sqrt{\lambda}=\gamma_1+i\gamma_2$, $\gamma_2\geqslant 0$. There results

$$\gamma p(\mathbf{x}) = p^0(\mathbf{x}) - \nabla \cdot \int\int_S \frac{\mathbf{t}(\mathbf{x}')\exp(ik|\mathbf{x}-\mathbf{x}'|)}{4\pi(1-i\omega\nu'/c_0^2)|\mathbf{x}-\mathbf{x}'|} da', \tag{A15}$$

$$\gamma \mathbf{v}(\mathbf{x}) = \mathbf{v}^0(\mathbf{x}) + \int\int_S \frac{\mathbf{t}(\mathbf{x}')\exp(ik^*|\mathbf{x}-\mathbf{x}'|)}{4\pi\rho_0\nu|\mathbf{x}-\mathbf{x}'|} da' + \nabla\nabla \cdot \int\int_S \times \frac{\mathbf{t}(\mathbf{x})\,[\exp(ik^*|\mathbf{x}-\mathbf{x}'|) - \exp(ik|\mathbf{x}-\mathbf{x}'|)]}{4\pi i\omega\rho_0|\mathbf{x}-\mathbf{x}'|} da' \tag{A16}$$

The function $\gamma(\mathbf{x})$ appears due to the known property of Fourier recovery of discontinuous furnctions. It has the expression

$$\gamma(\mathbf{x}) = \begin{cases} 1, & \text{for } \mathbf{x} \in \mathcal{D}^-, \\ 0.5, & \text{for } \mathbf{x} \in \mathcal{S}, \\ 0, & \text{for } \mathbf{x} \in \mathcal{D}^+. \end{cases}$$

The relationship (A16) is the *fundamental integral formula* for the motion of a compressible viscous fluid in a linear acoustic approximation.

[1]T. Chapman and B. Webb, "A neuromorphic hair sensor model of wind-mediated escape in the cricket," Int. J. Neural Syst. **9**, 397–403 (1999).
[2]J. Tautz, "Reception of particle oscillation in a medium-an unortodox sensory capacity," Naturwiss. **66**, 452–461 (1979).
[3]J. Tautz and H. Markl, "Catepillars detect flying wasps by hairs sensitive to airborne vibration," Behav. Ecol. Sociobiol. **4**, 101–110 (1978).
[4]N. H. Fletcher, "Acoustical response of hair receptors in insects," J. Comp. Physiol. **127**, 185–189 (1978).
[5]A. Reisland and P. Gorner, "Trichobothria," in *Neurobiology of Arachnids*, edited by F. G. Barth (Springer-Verlag, Berlin, 1985), pp. 138–161.
[6]F. G. Barth, *A Spider's World. Senses and Behavior* (Springer-Verlag, Berlin, 2002), p. 394.
[7]C. E. Bond, *Biology of Fishes*, 2nd ed. (Saunders College Publishing, Philadelphia, 1996).
[8]J. Mogdans, J. Engelmann, W. Hanke, and S. Krother, "The fish lateral line: How to detect hydrodynamic stimuli," in *Sensors and Sensing in Biology and Engineering*, edited by F. G. Barth, J. A. C. Humphrey, and T. W. Secomb (Springer-Verlag, Vienna, 2003), pp. 173–185.
[9]T. Shimozawa and M. Kanou, "Varieties of filiform hairs: range fractionation by sensory afferents and cercal interneurons of the cricket *Grillus Bimaculatus*," J. Comp. Physiol., A **155**, 495–505 (1984).
[10]I. Imai, "A new method of solving Oseen's equations and its application to the flow past an inclined elliptic cylinder," Proc. R. Soc. London, Ser. A **224**, 141–160 (1954).
[11]T. Kumagai, T. Shimozawa, and Y. Baba, "The shape of wind receptor hairs of cricket and cockroach," J. Comp. Physiol., A **183**, 187–192 (1998).
[12]J. A. C. Humphrey, R. Devarakonda, I. Iglesias, and F. G. Barth, "Dynamics of arthropod filiform hairs. I. Mathematical modeling of the hair and air motion," Philos. Trans. R. Soc. London, Ser. B **340**, 423–444 (1993).
[13]G. G. Stokes, "On the effect of the internal friction of fluids on the motion of pendulums," Trans Camb Phil Soc 9, 8ff (1851) [*reprinted in Mathematical and Physical Papers*, (Cambridge University Press, Cambridge, 1901), Vol. **III**, pp. 1–141.
[14]J. A. C. Humphrey, R. Devarakonda, I. Iglesias, and F. G. Barth, "Errata for dynamics of arthropod filiform hairs. I. Mathematical modeling of the hair and air motion," Philos. Trans. R. Soc. London, Ser. B **352**, 1995 (1997).
[15]J. A. C. Humphrey, R. Devarakonda, I. Iglesias, and F. G. Barth, "Errata for dynamics of arthropod filiform hairs. I. Mathematical modeling of the hair and air motion," Philos. Trans. R. Soc. London, Ser. B **353**, 2163 (1998).
[16]F. G. Barth, U. Wastl, J. A. C. Humphrey, and R. Devarakonda, "Dynamics of arthropod filiform hairs. III. Mechanical properties of spider trchobothria (*Cupiennius salei Keis.*)," Philos. Trans. R. Soc. London, Ser. B **340**, 445–461 (1993).
[17]F. G. Barth, J. A. C. Humphrey, J. Halbritter, and W. Brittinger, "Dynamics of arthropod filiform hairs. II. Flow patterns related to air movement detection in spider (*Cupiennius salei Keis.*)," Philos. Trans. R. Soc. London, Ser. B **347**, 397–412 (1995).
[18]R. Devarakonda, F. G. Barth, and J. A. C. Humphrey, "Dynamics of arthropod filiform hairs. IV. Hair motion in air and water," Philos. Trans. R. Soc. London, Ser. B **351**, 933–946 (1996).
[19]F. G. Barth and A. Holler, "Dynamics of arthropod filiform hairs. V. The response of spider tricobothria to natural stimuli," Philos. Trans. R. Soc. London, Ser. B **354**, 183–192 (1999).
[20]T. Shimozawa, T. Kumagai, and Y. Baba, "Structural scaling and function design of the cercal windreceptor hairs of cricket," J. Comp. Physiol., A **183**, 171–186 (1998).
[21]J. A. C. Humphrey, F. G. Barth, and K. Voss, "The motion-sensing hairs of Arthropods: using physics to understand sensory ecology and adaptive evolution," in *Ecology of Sensing*, edited by F. G. Barth and A. Schmid (Springer-Verlag, Berlin, Heidelberg 2001).
[22]J. A. C. Humphrey, F. G. Barth, M. Reed, and A. Spak, "The physics of Arthropod medium-flow sensitive hairs: biological models for artificial sensors," in *Sensors and Sensing in Biology and Engineering*, edited by F. G. Barth, J. A. C. Humphrey, and T. W. Secomb, (Springer-Verlag, Berlin 2003), pp. 129–144.
[23]T. Shimozawa, J. Murakami, and T. Kumagai, "Cricket wind receptors: thermal noise for the highest sensitivity known," in *Sensors and Sensing in Biology and Engineering*, edited by F. G. Barth, J. A. C. Humphrey, and T. W. Secomb (Springer-Verlag, Berlin, 2003).
[24]F. G. Barth and H-E Dechant, "Arthropod cuticular hairs: tactile sensors and refinement of stimulus transformation," 159–171.
[25]Y. Ozaki, T. Ohyama, T. Yasuda, and I. Shimoyama, "An air flow sensor modeled on wind receptor hairs of insects," *Proc. MEMS* 2000, Miazaki, Japan, pp. 531–537.
[26]J. Chen, Z. Fan, J. Engel, and C. Liu, "Two-dimensional micromachined flow sensor array for fluid mechanics studies," J. Aerosp. Eng. **16**, 85–97 (2003).
[27]Z. Fan, J. Chen, J. Zou, D. Bullen, C. Liu, and F. Delcomyn, "Design and fabrication of artificial lateral line flow sensors," J. Micromech. Microeng. **12**, 665–661 (2002).
[28]J. van Baar, M. Dijkstra, R. Wiegerink, T. Lammerink, R. de Boer, and G. Krijnen, "Artificial sensory hairs based on the flow sensitive receptor hairs of crickets," J. Micromech. Microeng. **15**, 132–138 (2005).
[29]J. Zou, J. Chen, and C. Liu, "Plastic deformation magnetic assembly (PDMA) of out-of-plane microstructures: technology and application," J. Microelectromech. Syst. **10**, 302–309 (2001).
[30]O. Rudko, M.Sc. thesis, State University of New York at Binghamton, "Design of a low-frequency sound sensor inspired by insect sensory hairs," Department of Mechanical Engineering, 2001.
[31]D. Homentcovschi and R. N. Miles, "Viscous scattering of a pressure wave by a hard body," submitted for publication.
[32]L. Dragos, *Mathematical Methods in Aerodynamics* (Springer-Verlag, Berlin, 2004).
[33]P. M. Morse and K. U. Ingard, *Theoretical Acoustics* (Princeton University Press, New Jersey, 1968).
[34]A. D. Pierce, *Acoustics* (McGraw-Hill, New York, 1981).
[35]L. D. Landau and E. M. Lifshitz, *Fluid Mechanics* (Pergamon, New York, 1959).
[36]I. Stakgold, *Boundary Value Problems of Mathematical Physics* (SIAM, Philadelphia, 2000).
[37]C. Pozrikidis, *Boundary Integral and Singularity Methods for Linearized Viscous Flow* (Cambridge University Press, Cambridge, 1992).
[38]W. Olmstead and A. K. Gautesen, "A new paradox in viscous hydrodynamics," Arch. Ration. Mech. Anal. **29**, 58–65 (1968).